

## Hot Paper

## Higher Assemblies of Coordination Cage-Catenanes Linked by Copper(II) Chloride Clusters: Networks and Transformations

Matthew P. Snelgrove,<sup>[a]</sup> Natalia N. Sergeeva,<sup>[b]</sup> and Michaele J. Hardie\*<sup>[a]</sup>

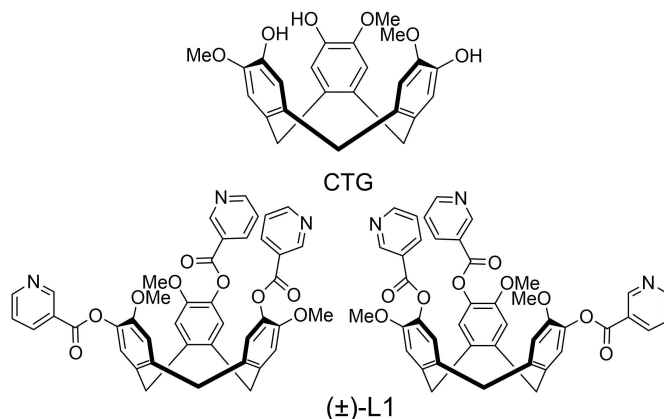
Cage-catenanes are chemical constructs where two or more cage-like molecules or assemblies are mechanically interlocked together. We report a new class of cage-catenanes where dimeric metal-organic cage-catenanes are linked into larger assemblies through additional bridging metal chloride links. These crystalline materials are obtained from the reaction of tris(nicotinoyl)cyclotruguaiacylene (L1) with Cu(II) salts, and all feature a tetramer of cages where two  $\{Cu_3(L1)_2(X)_6\}$  cages ( $X =$  anion) are mechanically interlocked, and link to each other and to another  $\{Cu_3(L1)_2(X)_6\}_2$  cage-catenane through a planar, linear

tetranuclear  $\{Cu_4(\mu-Cl)_6Cl_2\}$  cluster. The complex of discrete tetrameric  $\{Cu_3(L1)_2(X)_6\}_4$  assemblies (dimers of cage-catenanes) transforms through solvent-exchange processes to 1D coordination chain structures through additional  $\{Cu_2(\mu-Cl)_2\}$  bridges between the tetrameric  $\{Cu_3(L1)_2(X)_6\}_4$  assemblies. Complex  $[Cu_6(L1)_4Cl_{12}(H_2O)_3] \cdot (H_2O) \cdot 15(DMF)$  **C2** features a 2D coordination network of  $6^3$  topology linked through three different Cu(II) clusters, namely  $\{Cu_4(\mu-Cl)_6\}$ ,  $\{Cu_2(\mu-Cl)_2\}$  and a rare linear  $\{Cu_2(\mu-Cl)\}$  linkage. Break-down of **C2** in water likely proceeds through hydrolysis of this unusual linear Cu-Cl-Cl bond.

## Introduction

Metal-organic cages (MOCs, also known as coordination cages or metallocages) are discrete three-dimensional entities with inherent internal space. They are composed of bridging organic ligands brought together by coordination to metal centres. A rich chemistry of MOCs has developed addressing their synthesis, self-assembly behaviour, dynamic responses to external stimuli, and use as nanoscale molecular flasks, catalysts, sensors and therapeutics amongst other applications.<sup>[1]</sup>

Our work has focussed on the metallo-supramolecular chemistry of host-type ligands from the cyclotrimeratrylene (CTV) family.<sup>[2,3]</sup> CTV-type host molecules feature a tribenzo[*a,d,g*]cyclononene scaffold which usually adopts the crown conformation with a distinct bowl-shape with an open upper-rim and hydrophobic binding cavity.<sup>[4]</sup> Examples where the six upper rim substituents are not chemically identical, such as cyclotruguaiacylene (CTG, Scheme 1), are chiral, and there is a crown-saddle-crown racemisation pathway between enantiomers. Ligand-decorated CTV-analogues (here L-type ligands) are excellent building blocks for cage-assembly as they have an



Scheme 1. Cyclotruguaiacylene (CTG) and enantiomers of (tris(nicotinoyl)cyclotruguaiacylene, (±)-L1.

orthogonal arrangement of metal-binding groups and deep cavity. The smallest such cages are  $M_3L_2$  metallo-cryptophanes with a trigonal bipyramidal cage shape,<sup>[3,5,6]</sup> with the first examples reported by Yamaguchi and Shinkai.<sup>[5]</sup> They are analogues of organic cryptophanes, and, like the cryptophanes, can exist as achiral *syn* or chiral *anti* isomers due to chirality of the tripodal L-ligands.

Catenanes are a class of mechanically-interlocked molecules where two or more macrocyclic structures are inter-linked through a chain-like mechanical linkage. Topologically complex, interlocked chemical structures have intrinsic aesthetic appeal and have a myriad of potential applications ranging from catalysis to drug delivery to molecular electronics.<sup>[7]</sup> Metal-organic cages that are inter-locked to form catenane assemblies are a class of mechanically-interlocked molecules which has seen growing recent interest, including in: strategies for their synthesis; understanding and controlling the assembly of single

[a] Dr. M. P. Snelgrove, Prof. M. J. Hardie  
School of Chemistry  
University of Leeds  
Woodhouse Lane, Leeds LS2 9JT, UK  
E-mail: m.j.hardie@leeds.ac.uk

[b] Dr. N. N. Sergeeva  
School of Design  
University of Leeds  
Woodhouse Lane, Leeds LS2 9JT, UK

Supporting information for this article is available on the WWW under <https://doi.org/10.1002/chem.202403692>

© 2024 The Author(s). Chemistry - A European Journal published by Wiley-VCH GmbH. This is an open access article under the terms of the Creative Commons Attribution License, which permits use, distribution and reproduction in any medium, provided the original work is properly cited.

cage or catenane and their transformations; and their host-guest binding and release behaviour.<sup>[8–14]</sup> Cage-catenane MOCs were first documented by Fujita in 1999 who reported triply interlocked cages of two  $[M_3L_aL_b]$  cages where  $L_a/L_b$  were chemically-distinct tripodal bridging ligands.<sup>[10]</sup> It was nearly 10 years before other examples emerged,<sup>[11,12]</sup> including our own report of a triply-interlocked metallo-cryptophane from a 2,2'-bipyridine-decorated cyclotriguaiacylene ligand,<sup>[12]</sup> and we subsequently reported a  $\{Ag_3L_2\}_2$  cage-catenane where  $L = \text{tris}(3\text{-pyridylmethyl})\text{cyclotriguaiacylene}$ .<sup>[13]</sup> Cage-catenanes can also result from assembly of purely organic cages.<sup>[8]</sup>

Most examples of cage-catenanes are discrete entities. Exceptions to this including crystalline 3D arrays of adamantane-shaped metal-organic cages where each cage interlocks with six others,<sup>[14]</sup> 3D arrays of tetrahedral MOCs,<sup>[15]</sup> and 1D assemblies where each cage interlocks with two others to form a linear chain.<sup>[15,16]</sup> These represent a highly unusual class of coordination polymer/metal-organic framework where the polycatenation of discrete cages results in an extended network. Higher level assemblies of cage-catenanes through supramolecular interactions has resulted in crystalline materials with lattice void spaces,<sup>[17]</sup> and aggregation into larger nanostructures is also known.<sup>[18]</sup>

We report herein a distinct class of higher assemblies of interlinked metal-organic cages with both 1D and 2D coordination polymer motifs. Here, rather than polymerisation through poly-catenation, extended networks are propagated through bridging metal chloride clusters that occur between the MOCs. The metal-organic cages are  $M_3L_2$  metallo-cryptophane moieties from ligand  $(\pm)\text{-}2,7,12\text{-trimethoxy-}3,8,13\text{-tris}(3\text{-pyridylcarboxy})\text{-}10,15\text{-dihydro-}5H\text{-tribenzo}[a,d,g]\text{cyclononene}$  (*tris*(nicotinoyl)cyclotriguaiacylene,  $(\pm)\text{-}L1$ , Scheme 1). Interestingly, while the synthesis of ligand L1 was reported as far back as 2004,<sup>[19]</sup> this is the first report of a metallo-supramolecular derivative of it. This is in stark contrast with its isomer *tris*(isonicotinoyl)cyclotriguaiacylene which is found in coordination polymers<sup>[2]</sup> and various classes of MOCs.<sup>[3]</sup>

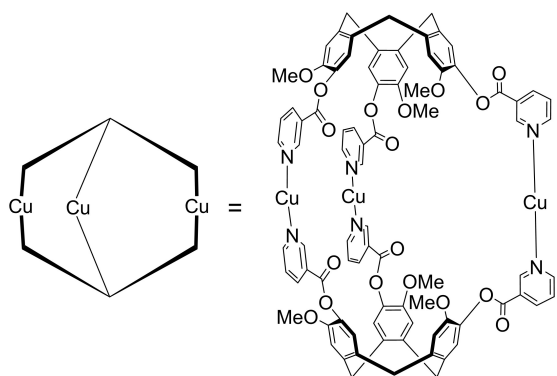
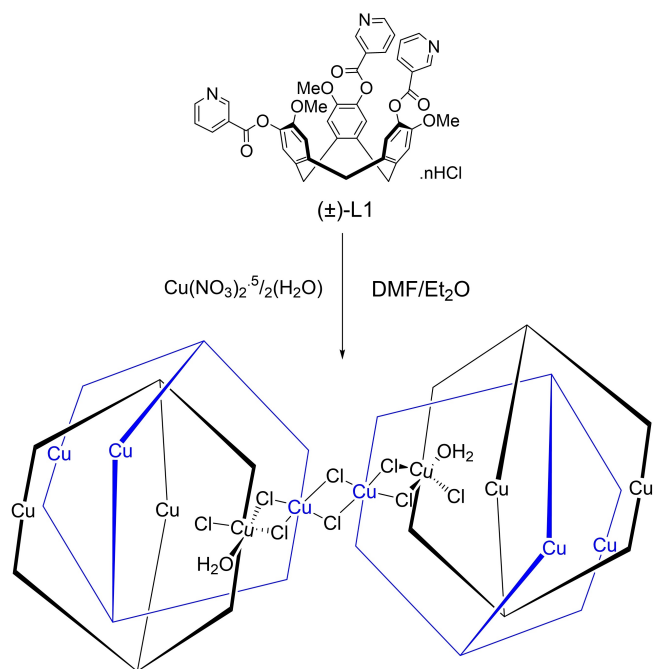
## Results and Discussion

Reaction of ligand  $(\pm)\text{-}L1$  with  $\text{Cu}(\text{NO}_3)_2$  in dimethylformamide (DMF) gave low yields of single crystals through vapour diffusion with diethyl ether. Single crystal X-ray analysis indicated that their composition is  $[\text{Cu}_6(\text{L}1)_4\text{Cl}_{10.5}(\text{NO}_3)_{1.5}(\text{H}_2\text{O})_4]\cdot n(\text{DMF})$  **C1**.<sup>[20]</sup> The presence of chloride anions was corroborated by Energy Dispersive X-Ray (EDX) analysis (see section 3.1 of supplementary information, SI). Stretching frequencies attributable to nitrate anions were observed in infrared spectra at 1324 and 1386  $\text{cm}^{-1}$  (Figure S12, SI). The source of the chloride is likely to be the L1 ligand, whose synthesis involves use of the hydrochloride salt of nicotinoyl chloride.<sup>[19]</sup> Despite use of an excess of base during synthesis of L1, a small % of the hydrochloride salt of L1 is present, also confirmed by EDX (SI section 3.1.1) which indicates that only a small amount of Cl needs to be present for **C1** to form. We have previously reported the adventitious incorpo-

ration of chloride contaminant from a related CTV-type ligand in the synthesis of a Ag-Cl linked coordination polymer.<sup>[21]</sup> Synthesis of **C1** is repeatable and a single crystal structure of **C1** obtained using a different batch of  $(\pm)\text{-}L1$  was isostructural with that described below (see information for **C1** “batch B” single crystal structure in Table S1 and Figures S2 and S3 in SI for details). Unit cell determinations were undertaken on multiple crystals from different synthetic batches of both ligand and **C1** synthesis, and all were consistent (Table S2, SI).

The crystal structure of **C1** was solved in space group  $P\bar{1}$  and features dimeric cage-catenanes with two interlocked  $\{\text{Cu}_3(\text{L}1)_2\}$  metallo-cryptophanes forming the asymmetric unit of the structure. There are six different Cu(II) coordination environments, all of which feature a *trans* arrangement of coordinating pyridyls from two L1 ligands at Cu-N distances ranging from 1.975(8) to 2.044(9) Å. Each Cu(II) has additional equatorial chloride, nitrate and/or aquo ligands. Four of the six Cu(II) centres have 5-coordinate trigonal bipyramidal or square pyramidal geometry. One metallo-cryptophane cage has composition  $[\{\text{CuCl}_2(\text{H}_2\text{O})\}_3(\text{L}1)_2]$  with aquo and chloro ligands, while the other has composition  $\{\text{Cu}_3\text{Cl}_{4.5}(\text{NO}_3)_{1.5}(\text{H}_2\text{O})_2(\text{L}1)_2\}$  and two of the three Cu(III) centres are coordinated by nitrate as well as chloro counter-anions, with  $\text{NO}_3/\text{Cl}$  disorder apparent for one Cu(II). Each metallo-cryptophane cage is the achiral *syn* isomer with both ligand enantiomers present. As with other examples of metallo-cryptophane-based cage-catenanes, each cage is interlocked with the other in a triply interlocked manner. The central cavity of the cage-catenane is approximately 230 Å<sup>3</sup>. Face-to-face  $\pi\text{-}\pi$  stacking interactions occur between pyridyl rings of different cages. Unlike most other examples of cage-catenanes where the two cages are fully independent of one another,<sup>[22]</sup> the cages here are chemically linked through  $\text{Cu}(\mu\text{-Cl})_2\text{-Cu}$  bridges. Each bridging  $\text{Cl}^-$  shows a short Cu-Cl bond length at 2.293(2) or 2.323(3) Å and a longer interaction bridging to the Cu(II) centre of the other cage at 2.890(3) or 2.937(3) Å. Chloride bridges extend to link to a second cage-catenane related to the first through an inversion centre, forming a linear tetranuclear  $\{\text{Cu}_4(\mu\text{-Cl})_6\text{Cl}_2(\text{OH}_2)_2\}$  cluster. Each Cu(II) centre within the cluster is also coordinated by *trans* pyridyl groups of the L1 ligands (Cu-N distances 1.986(10) to 2.018(8) Å) hence has a distorted octahedral geometry with a significantly elongated axis consistent with Jahn-Teller elongation (elongated axes: Cu-Cl distances 2.890(3) to 2.937(3) Å, Cu-O 2.455(8) Å; other axes Cu-Cl 2.283(4) to 2.323(3) Å). Cu...Cu distances within the tetramer are 3.743 and 3.778 Å. The pyridyl groups associated with this cluster show face-to-face  $\pi\text{-}\pi$  stacking interactions at ring centroid separations ranging from ca. 3.68 to 3.76 Å. Hence a tetrameric cage assembly which is a dimer of dimeric cage-catenanes is formed, Scheme 2 and Figure 1, which is a motif that has not been previously reported for coordination cages.

The flat, linear tetranuclear Cu(II) cluster motif displayed by **C1** is also highly unusual. Similar discrete linear doubly chloro-bridged tetranuclear clusters of *trans*-octahedral Cu(II) have not been previously reported, and, to the best of our knowledge, this represents a new class of small Cu-clusters. Flat, linear tetranuclear clusters with octahedral metal centres have been



**Scheme 2.** Synthesis of crystalline material complex **C1** with achiral *syn* cages shown in cartoon form. Terminal  $\text{H}_2\text{O}$ ,  $\text{NO}_3^-$  and  $\text{Cl}^-$  groups ligated to the Cu(II) centres that are not involved in Cu-cluster formation have been omitted for clarity. The blue and black cages are chemically distinct, with variations in these terminal ligands (see Figure 1).

reported for  $[\text{Fe}_4(\mu\text{-Cl})_6(\text{H}_2\text{O})_{12}]^{2+}$ <sup>[23]</sup> along with a near-planar analogue in  $[\text{Mn}_4(\mu\text{-Cl})_6\text{Cl}_4(\text{H}_2\text{O})_8]^{2-}$ <sup>[24]</sup>. The closest parallels in copper chemistry are doubly chloro-bridged  $[\text{Cu}_4\text{Cl}_n]$  clusters with square planar/square pyramidal Cu(II) centres,<sup>[25]</sup>  $[\text{Cu}_4(\mu\text{-Cl})_6\text{Cl}_2\text{L}_2]$  complexes where zig-zagging tetranuclear clusters with 5-coordinate metal geometry which are end-capped by chelating or macrocyclic ligands,<sup>[26]</sup> infinite doubly chloro-bridged  $[\text{Cu}_n\text{Cl}_m(\text{H}_2\text{O})_p]^{x-}$  chains with octahedral coordination,<sup>[27]</sup> and an infinite  $[\text{Cu}(\mu\text{-Cl})_3]^-$  anion with triply chloro-bridged structure with octahedral metal geometry and a linear chain structure.<sup>[28]</sup> The Cu-Cl distances of the Jahn-Teller elongated axis of the  $[\text{Cu}(\mu\text{-Cl})_3]^-$  chain, for example, are consistent with those found in complex **C1**. Complex  $[\text{Cu}(\text{bp3ca})\text{Br}_2]$  (where

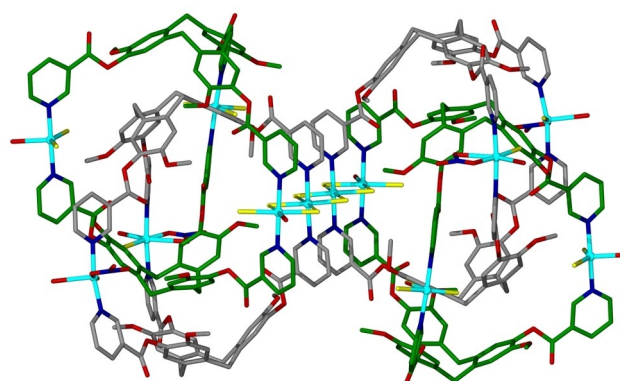


**Figure 1.** Dimer of two  $\{\text{Cu}_3(\text{L1})_2\}$  cage-catenanes from the crystal structure of **C1**. The tetrameric metallo-cryptophane assembly is linked through a linear tetranuclear  $\{\text{Cu}_4(\mu\text{-Cl})_6\text{Cl}_2(\text{OH}_2)_2\}$  cluster. Hydrogen atoms excluded for the sake of clarity. Grey = C; red = O; dark blue = N; yellow = Cl; light blue = Cu.

$\text{bp3ca} = 2,2'$ -bipyridine-3,3'-dicarboxylic acid) also features a tetranuclear, doubly halide-bridged structure with long and short Cu-Br bridges. There, however, the distorted octahedral Cu(II) centres have a zig-zag rather than linear aspect with the chelating bp3ca ligand occupying *cis*-coordination positions.<sup>[29]</sup> Packing of the neutrally charged  $[\text{Cu}_6(\text{L1})_4\text{Cl}_{10.5}(\text{NO}_3)_{1.5}(\text{H}_2\text{O})_4]$  tetrameric (dimer of dimers) cage-catenanes in the crystal lattice does not fill space and there are significant channels apparent in the lattice when viewed down both the *b* and *c* axes, Figure 2. The solvent-accessible void in the lattice is approximately 60% of the volume. A sphere of radius 4.60 Å could penetrate the *b* direction, while one of radius 4.20 Å could penetrate the *c* axis, determined using void analysis protocols in Olex-2.<sup>[30]</sup> These channels are filled with dimethylformamide whose locations could not be resolved in the crystal structure, but whose presence is indicated by infrared spectroscopy (Figure S12) and thermogravimetric analysis (TGA), Figure S16 SI. Solvation level estimated from TGA is  $[\text{Cu}_6(\text{L1})_4\text{Cl}_{10.5}(\text{NO}_3)_{1.5}(\text{H}_2\text{O})_4] \cdot 17(\text{DMF})$ . The material is not robust and significant cracking and sintering of crystals occurs if they are removed from their mother liquor. Washing with dichloromethane, followed by drying *in vacuo* results in the formation of amorphous material as shown the powder XRD pattern, Figure S11 SI. Once formed, the crystals were not readily soluble in DMF, however immersion in water lead to rapid breakdown of the crystals. The mass spectrum of a DMF-mixture of  $\text{Cu}(\text{NO}_3)_2$  and  $(\pm)\text{-L1}$  obtained prior to crystallisation of **C1** gave no indication that the cage-catenane structures are formed in solution, with the spectra dominated by ligand peaks, see Figure S14 in SI.

Despite the fragility of the crystals when removed from mother liquor, they remain stable when kept under solvent. The material was therefore investigated for potential uptake of guest molecules from solution. Given the large size of the channels, samples of as-synthesised **C1** were soaked in toluene solutions of fullerenes  $\text{C}_{60}$  and of  $\text{C}_{70}$  in separate experiments, following our previous report of fullerene-uptake by a 2D Cu(II) coordination polymer composed of network metallo-



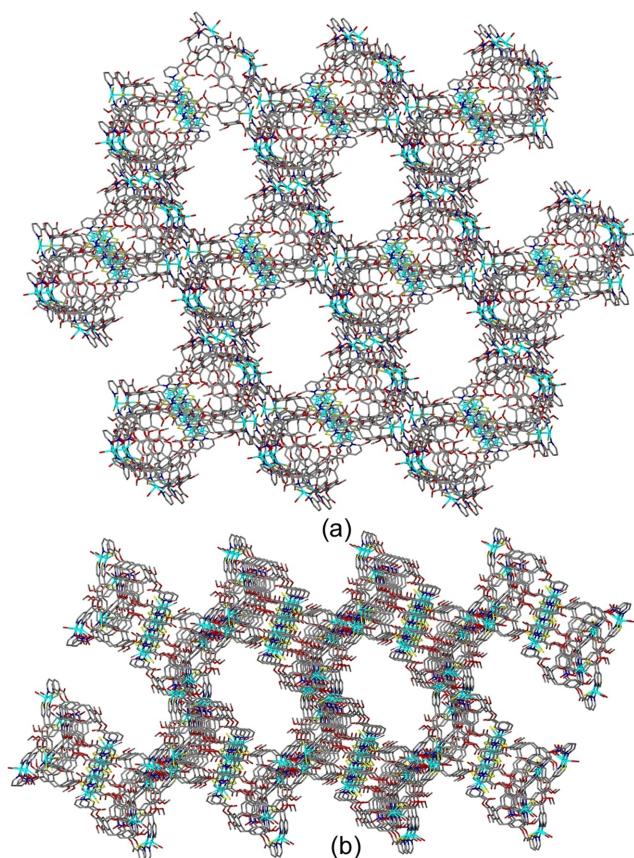
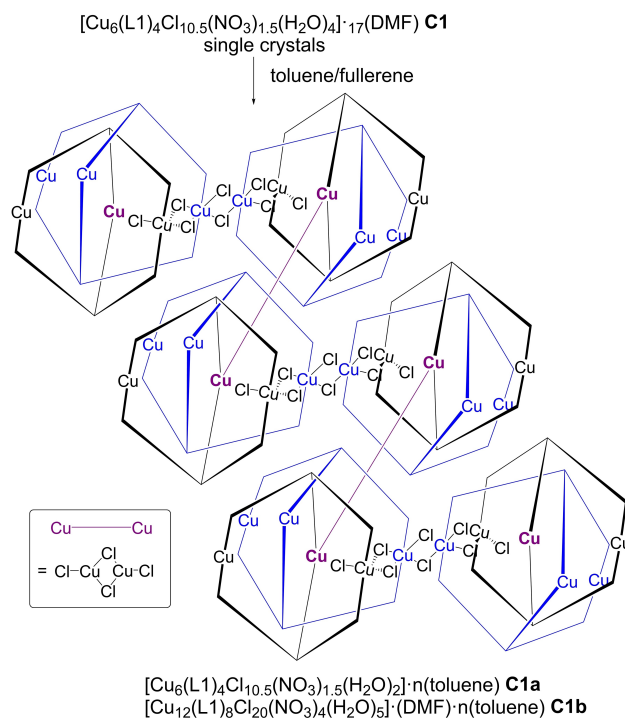


**Figure 2.** Crystal packing of **C1** viewed down (a) *b* axis and (b) *c* axis showing solvent-filled large channels.

cryptophanes.<sup>[31]</sup> There was no indication that fullerenes were absorbed by **C1**, however both batches of material remained as largely single crystals hence their single crystal structures were obtained.

There were two materials identified in each batch, namely:  $[\text{Cu}_6(\text{L}1)_4\text{Cl}_{10.5}(\text{NO}_3)_{1.5}(\text{H}_2\text{O})_2] \cdot n(\text{toluene})$  **C1a** and  $[\text{Cu}_{12}(\text{L}1)_8\text{Cl}_{20}(\text{NO}_3)_4(\text{H}_2\text{O})_5] \cdot (\text{DMF}) \cdot n(\text{toluene})$  **C1b**,<sup>[20]</sup> which both featured very similar coordination chain structures, Scheme 3. Both experiments yielded crystals of both **C1a** and **C1b**. According to unit cell determinations, of 17 single crystals sampled, 52% were **C1a** (Table S3, SI). The crystal quality of **C1b** was routinely poorer than that of **C1a** and nominally single crystals of **C1b** had a multi-crystal component with only ca. 80% of reflections indexing to the dominant lattice. Single crystal X-ray structures could be obtained of both materials. The structures of **C1a** and **C1b** are very closely related and both feature the tetranuclear Cu(II) cluster linking cage-catenanes seen in **C1**. In both cases it is apparent that toluene is present within the crystal lattice, and this solvent exchange process is concomitant with significant structural differences from the parent **C1** complex.

Complex **C1a** is triclinic with smaller unit cell volume of 13263.9(6) Å<sup>3</sup> compared with 17806.2(8) Å<sup>3</sup> for **C1**. The structure was also solved in space group  $P\bar{1}$ . The asymmetric unit of **C1a** is similar to that of **C1** and it is notable that the positions of two



**Scheme 3.** Synthesis of complexes **C1a** and **C1b** from **C1** with formation of polymeric chain motif from additional Cu-Cl dimerization shown in cartoon form at Cu centres indicated in purple. Cage cartoon and colour coding is the same as for Scheme 2.

toluene molecules could be established, Figure 3b. For much of the assembly the differences between **C1a** and parent **C1** are relatively minor and pertain to nuances of the coordination geometry, and orientation of the L1 nicotinoyl groups, Figure 3. For example, the Cl-Cu-Cl angle on Cu2 is somewhat straighter for **C1a** at 158.2(5)° than for **C1** at 147.07(16)°. There are more significant differences at Cu3 and Cu1. The terminal aquo ligand on the Jahn-Teller elongated octahedral axis of Cu3 in **C1** is missing from **C1a** where the equivalent Cu3 has square pyramidal coordination. Instead, a toluene molecule is located in proximity to that coordination site, with closest contact C-H...Cu3 at 3.71 Å. Cu1 in **C1** has square planar coordination geometry where the apical and one basal ligand are of mixed Cl<sup>-</sup>/H<sub>2</sub>O character. This is significantly altered in **C1a** where the asymmetric unit has square planar coordination with two *trans* ordered Cl<sup>-</sup> ligands rotated approximately 90° compared with the *trans* basal Cl/H<sub>2</sub>O ligands of **C1**. Cu1 is close to an inversion centre and the full coordination geometry of Cu1 is shown in inset box of Figure 3b, where it can be seen that Cu1 has square pyramidal geometry and forms a doubly chloride-bridged [Cu<sub>2</sub>(μ-Cl)<sub>2</sub>Cl<sub>2</sub>] dimer. The bridging Cu-Cl distances are 2.313(2) and 2.639(2) Å. Cu5 is also sited close to an inversion centre over which the tetranuclear [Cu<sub>4</sub>(μ-Cl)<sub>6</sub>Cl<sub>2</sub>] cluster is formed. Here, Cu3 has square pyramidal geometry, while Cu5 is octahedral with bridging chlorides on the Jahn-Teller elongated axis (Cu-Cl 2.848(3), 2.961(3) Å) other bridging Cu-Cl distances in the cluster are 2.289(3), 2.314(3), 2.306(3), and 2.642(3) for the apical position on square pyramidal Cu3. Thus, there is

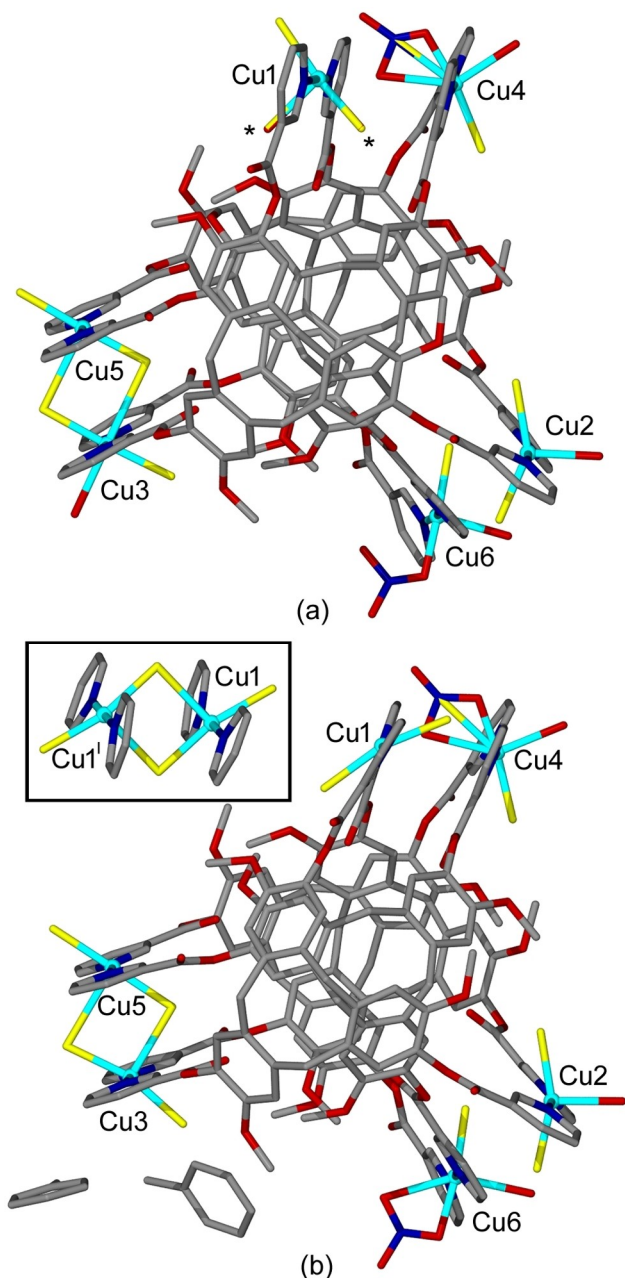


**Figure 3.** Asymmetric units of the crystal structures of (a) **C1** and (b) **C1a**. Ligand positions marked with an asterisk were refined as mixed Cl/H<sub>2</sub>O. Cu4 of both structures has one coordinating anion modelled as disordered Cl/NO<sub>3</sub> each at 50% occupancy. Box shows full coordination geometry for Cu1 in **C1a**. Symmetry operator I: 2-X,2-Y,1-Z. Hydrogen atoms excluded for the sake of clarity.

chloride bridging between the dimeric cage-catenanes at two crystallographically inequivalent Cu-sites in complex **C1a** – at sites Cu1 and Cu5 – resulting in formation of a coordination chain structure.

Two adjacent [Cu<sub>6</sub>(L1)<sub>4</sub>Cl<sub>10.5</sub>(NO<sub>3</sub>)<sub>1.5</sub>(H<sub>2</sub>O)<sub>2</sub>] coordination chains of complex **C1a** and an expansion of the dinuclear [Cu<sub>2</sub>(μ-Cl)<sub>2</sub>Cl<sub>2</sub>] cluster linking two metallo-cryptophane cage-catenanes are shown in Figure 4a. As for the tetranuclear cluster, the pyridyl groups coordinating to the dinuclear [Cu<sub>2</sub>(μ-

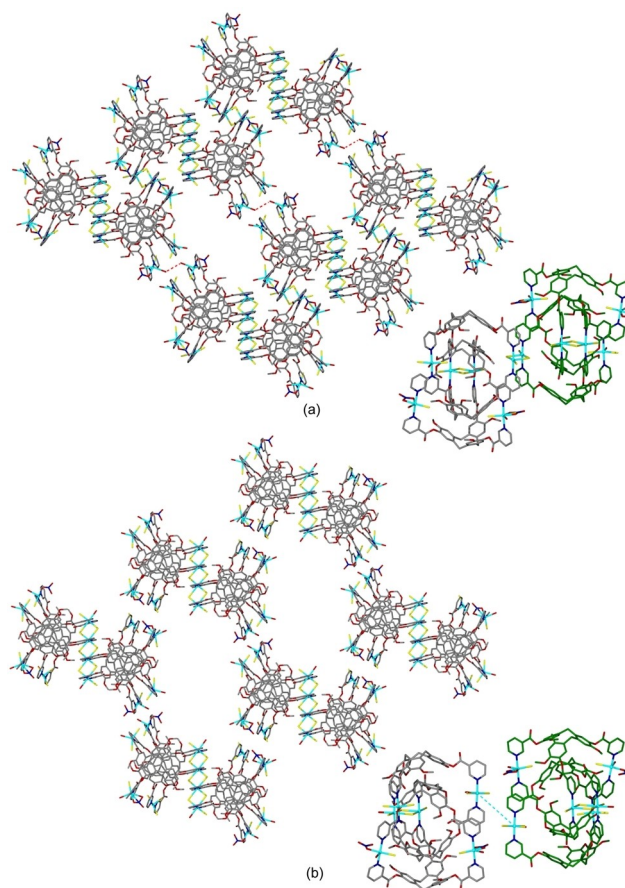


**Figure 4.** (a) Section of crystal structure of **C1a** showing packing of adjacent coordination chains in 2D with intra-chain hydrogen bonding indicated as dashed red line and (right) expanded side-view of two cage-catenanes within a chain that are linked by the dinuclear [Cu<sub>2</sub>(μ-Cl)<sub>2</sub>Cl<sub>2</sub>] motif. (b) Equivalent packing view of **C1** with (right) expanded side-view of the equivalent cage-catenanes shown in expansion in (a) with dashed blue line indicating the two Cu1 centres equivalent to those that form the dinuclear cluster in **C1a**.

Cl)<sub>2</sub>Cl<sub>2</sub>] cluster form face-to-face π-π stacking interactions, with a centroid separation of 3.59 Å. Each coordination chain forms hydrogen bonding interactions to two symmetry equivalent coordination chains through aquo ligands coordinated to Cu6, with O...O separation of 3.29 Å to form a 2D network, Figure 4a. If each {Cu<sub>3</sub>(L)<sub>2</sub>} cage-catenane is regarded as a structural node, then the combination of coordinate and hydrogen bonding interactions between them gives a network of 6<sup>3</sup> topology. The network features distorted hexagonal cavities of approximately 9 x 24 Å cross-section which contain solvent molecules. Figure 4b shows how the discrete [Cu<sub>6</sub>(L1)<sub>4</sub>Cl<sub>10.5</sub>(NO<sub>3</sub>)<sub>1.5</sub>(H<sub>2</sub>O)<sub>4</sub>] molecules of the parent **C1** pack in 2D when viewed in a similar orientation to the 2D network of **C1a**. The packing in 2D is notably similar, albeit with larger hexagonal cavities for **C1**. The symmetry-equivalent Cu(II) centres that form the [Cu<sub>2</sub>(μ-Cl)<sub>2</sub>Cl<sub>2</sub>] clusters in **C1a** (designated Cu1) are facing one another in **C1** highlighted in the side-on view of two metallo-cryptophanes in Figure 4b. These Cu1 centres are 7.45 Å apart in **C1** (dashed line Figure 4b), compared with 3.52 Å separation in the [Cu<sub>2</sub>(μ-Cl)<sub>2</sub>Cl<sub>2</sub>] dimer of **C1a**. There



are no hydrogen bonds between adjacent cage-catenanes as seen in **C1a**, with the equivalent aquo ligands on Cu6 5.74 Å apart (O...O separation) and significantly out-of-plane with respect to one another. Any transformation of the discrete  $[\text{Cu}_6(\text{L}1)_4\text{Cl}_{10.5}(\text{NO}_3)_{1.5}(\text{H}_2\text{O})_4]$  to the 1D chain  $[\text{Cu}_6(\text{L}1)_4\text{Cl}_{10.5}(\text{NO}_3)_{1.5}(\text{H}_2\text{O})_2]$  is not through a simple translation along the Cu1...Cu1 vector shown in Figure 4b but requires more complex translations along with loss of aquo ligand on Cu1 and chloro ligand rotations (see Figure S4 in SI). The 3D packing between layers in **C1a** is distinct to that of **C1** with smaller channels in the *b* axis (Figure S5). The solvent-accessible void space is ca. 48% of unit cell volume and the largest penetrating sphere is 3.00 Å along the *b* axis (calculated without solvent molecules in lattice). Comparison with solvation levels of **C1** along with mask/void calculations for **C1a** indicated space for 15 toluene molecules per asymmetric unit in **C1a**, however a mixture of toluene and DMF guest solvent cannot be ruled out.

Complex **C1b** is very similar to **C1a**. It crystallises in a larger triclinic unit cell and the asymmetric unit is double the size of that of **C1a** with two cage-catenanes linked by the  $[\text{Cu}_2(\mu\text{-Cl})_2\text{Cl}_2]$  dimer (Figure S6). The larger asymmetric unit can be accounted for by there being two chemically distinct bridging Cu(II)-tetranuclear clusters. One has the same  $\{\text{Cu}_4(\mu\text{-Cl})_6\text{Cl}_2\}$  form as seen in **C1a**, with terminal chloro ligands and a toluene solvate molecule close-by at C—H...Cu distance 3.83 Å. The other is  $\{\text{Cu}_4(\mu\text{-Cl})_6(\text{NO}_3)_2\}$  with terminal nitrate ligands, rather than the terminal chloro, Figure 5. Orientation of some methoxy groups of the L1 ligands are different for the two cage-catenanes and there is some disorder of one nicotinoyl group that was not apparent in **C1a**, along with some disorder of chloro ligands. One coordinated nitrate position could not be refined, although it was apparent in the difference map. A dimethylformamide solvent along with toluene were located in the unit cell. Otherwise, the structures of **C1a** and **C1b** are very similar throughout the respective lattices. Complex **C1b** also features 2D hydrogen-bonded layers of the tetranuclear/dinuclear-linked coordination chain forming, albeit with one ligand involved in intra-chain hydrogen-bonding refined as

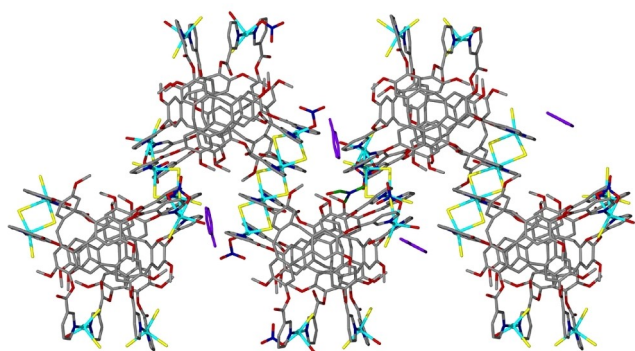


**Figure 5.** Section of the coordination chain structure of **C1b** highlighting the two types of  $\{\text{Cu}_4(\mu\text{-Cl})_6\}$  cluster found, one capped with terminal nitrate ligands, the other with chloro ligands. Toluene molecules are shown in purple, and C of DMF in green. Disorder position of one nicotinoyl and hydrogen atoms excluded for clarity.

partially occupied chloride, which is consistent with larger distance between the chains (3.49 *cf.* 3.29 Å), Figure S7 (SI). The 3D packing motifs are also very similar (Figure S8).

Solvent-induced structural changes in coordination complexes,<sup>[32]</sup> including in coordination polymers,<sup>[33,34]</sup> are relatively common and examples where the nuclearity of metal clusters is increased, as here, have been reported.<sup>[35]</sup> Externally-induced structural transitions in coordination polymers may occur as solid-state single-crystal-to-single-crystal transformations or through solvent-mediated crystal-to-crystal processes which may involve epitaxial crystal growth associated with microscopic dissolution and crystallisation processes.<sup>[36]</sup> Optical microscopy of **C1a** and **C1b** samples compared with the parent **C1** reveals visible deterioration in crystal quality despite single crystal diffraction data being obtainable from these samples (Figure S1). This suggests that the structural changes observed may not be occurring in a strictly solid-state process. Attempts to measure the unit cell parameters of an individual crystal of **C1** in its as-synthesised state as well as after soaking in toluene were unsuccessful with repeated cooling/thawing/handling and X-ray exposure resulting in further degradation.

As synthesis of **C1** relied on adventitious chloride, ( $\pm$ )-L1 was deliberately reacted with  $\text{CuCl}_2 \cdot 6\text{H}_2\text{O}$  in a similar manner. After two weeks this gave crystals of composition  $[\text{Cu}_6(\text{L}1)_4\text{Cl}_{12}(\text{H}_2\text{O})_3] \cdot (\text{H}_2\text{O}) \cdot 15(\text{DMF})$  **C2** (Scheme S1 in SI) with solvation levels estimated from solvent mask. The presence of DMF was also indicated by infrared spectroscopy (Figure S13). As for **C1**, the DMF reaction solution prior to crystallisation was probed by mass spectrometry, which gave no evidence of a Cu(II) complex being formed in solution, and was dominated by ligand peaks, Figure S15. Material **C2** was obtained in over double the yield than was **C1**. Complex **C2** crystallised in a triclinic unit cell distinct from those of **C1**, **C1a** or **C1b** (Table 1) and its structure solved in space group  $P\bar{1}$ .<sup>[20]</sup> The unit cell parameters are most comparable to those of **C1a** being similar in the *a* and *c* axes though approximately 12% larger for the *b* axis. The asymmetric unit is shown in Figure 6 and as expected, shows only chloride counter-anions are present. As before, two *syn* isomer  $\{\text{Cu}_3(\text{L}1)_2\}$  metallo-cryptophanes are formed and these interlock into a cage-catenane assembly where the two cages are chemically bound through bridging  $\text{Cu}(\mu\text{-Cl})_2\text{-Cu}$

**Table 1.** Unit cell parameters of materials.

	<i>a</i> (Å) $\alpha$ (°)	<i>b</i> (Å) $\beta$ (°)	<i>c</i> (Å) $\gamma$ (°)
<b>C1</b>	26.3309(7) 91.650(2)	27.3750(6) 116.006(2)	29.8979(6) 109.881(2)
<b>C1a</b>	20.6704(5) 98.692(2)	22.3503(6) 104.319(2)	30.1204(7) 93.24(2)
<b>C1b</b>	22.3579(5) 68.887(3)	32.0688(9) 87.309(2)	39.9945(11) 79.769(3)
<b>C2</b>	20.2327(7) 73.824(3)	25.1322(8) 77.190(3)	29.8112(9) 79.769(3)
<b>C2W<sup>(a)</sup></b>	20.49(1) 99.21(1)	22.43(1) 104.37(1)	29.88(1) 92.16(1)

[a] single crystal fragment from **C2** soaked in water, estimated esds.

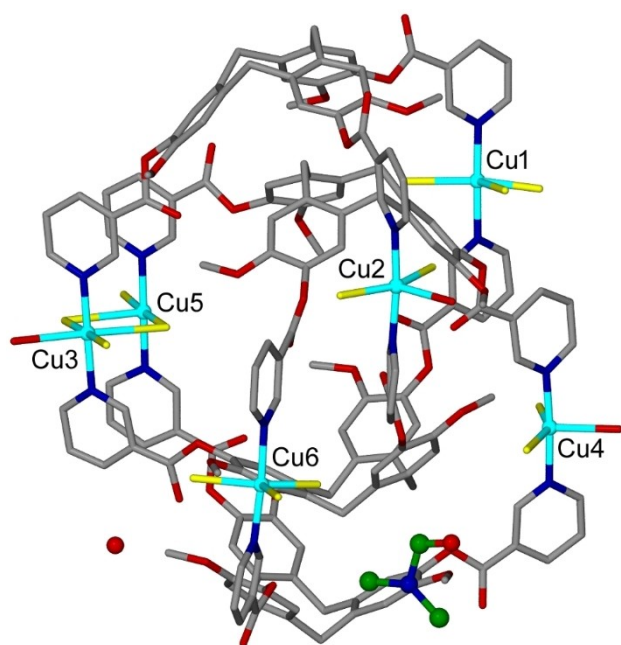


**Figure 6.** Asymmetric unit of the crystal structure of  $[\text{Cu}_6(\text{L}1)_4\text{Cl}_{12}(\text{H}_2\text{O})_3] \cdot (\text{H}_2\text{O})_n(\text{DMF})$  **C2**. DMF shown with C in green. Cu numbering is matched to similar Cu centres in **C1** family of complexes. One of the  $\text{Cl}^-$  coordinated to each of Cu1 and Cu6 are disordered across two sites. Hydrogen atoms not shown for clarity.

links, Figure 6. There are six 5- or 6-coordinate Cu(II) environments, three with a terminal aquo ligand alongside terminal or bridging chloro ligands, and three only coordinated by chloro ligands. One terminal chloro ligand of Cu1 was disordered across two sites, and one chloro coordinated to Cu6 refined at half occupancy. One DMF and a water solvent molecule were located in the lattice.

As for the **C1** family of complexes, two cage-catenanes are linked together through a flat tetranuclear doubly-chloro bridged cluster (Figure 7) in this case with terminal aquo

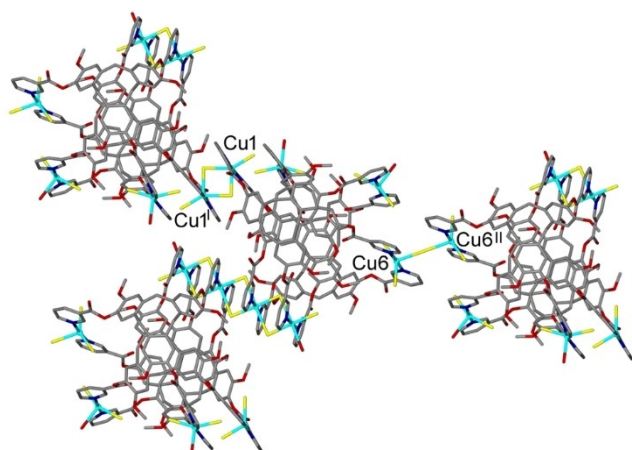


**Figure 7.** Cu(II) coordination environments in **C2**. Only the major Cl disorder position is shown for the disordered terminal Cl of Cu1. The linear bridging chloro of Cu6 is sited on an inversion centre. Symmetry operators: I-X, -Y-1, 3-Z; II 1-X, -Y, 2-Z.

ligands at Cu-O distance 2.545(11) Å. The  $\{\text{Cu}_4(\mu\text{-Cl})_6\text{Cl}_2(\text{OH}_2)_2\}$  cluster has short bridging Cu-Cl distances ranging from 2.297(3) to 2.326(4) Å and longer bridging distances between 2.848(4) and 2.872(3) Å. Two other Cu(II) centres of the asymmetric unit are connected to symmetry-equivalent Cu(II) centres through chloro-bridges. For Cu1 this is a  $[\text{Cu}_2(\mu\text{-Cl})_6\text{Cl}_2]$  dimeric cluster similar to that observed in **C1a/b**. The terminal chloro of the cluster is disordered across two positions and only the site with higher occupancy is shown in Figures 7 and 8, which gives Cu1 a trigonal bipyramidal geometry rather than the square pyramid adopted by Cu1 sites in **C1a** and **C1b**. Bridging Cu1-Cl distances are 2.428(3) and 2.535(3) Å.

Cu6 is involved in a much more unusual bridging motif, forming a linear singly-bridged Cu-Cl-Cu unit. The bridging chloro ligand is sited on an inversion centre, hence the Cu-Cl-Cu angle is  $180^\circ$  and the Cu-Cl distance is 2.5752(18) Å. While unusual, this is not unprecedented, and a handful of complexes with linear or near-linear Cu(II)-Cl-Cu(II) motifs have been reported<sup>[37,38]</sup> and the bond lengths found here are consistent with the majority of those reports.<sup>[37]</sup> The only prior report of such a motif in a coordination polymer showed a considerably longer Cu-Cl length of 3.024 Å.<sup>[38]</sup> Each cage-catenane in **C2** is coordinated to three others through three chemically-distinct chloro-bridged clusters to form a 2D coordination polymer.

The 2D coordination polymer has  $6^3$  topology if each  $\{\text{Cu}_3(\text{L}1)_2\}_2$  cage-catenane is considered a network connecting node, Figure 8. It is similar to the 2D network of hydrogen-bonded coordination chains of **C1a/C1b** where the linear Cu-Cl-Cu linkage at Cu6 replaces hydrogen bonding between aquo ligands bonding bridges that occurred at the Cu6 positions of **C1a**. The layers pack to produce similar channels along the *b* axis as seen in the other complexes, and also show channels in other directions (Figures S9, S10 SI). Overall, the solvent-filled space within the lattice is smaller than that of **C1**.

Complex **C2** was assessed for potential application in the photocatalytic degradation of dyes, noting there are other examples of Cu(II)-coordination polymer materials used for such purposes.<sup>[39]</sup> Very modest effects were seen with methyl orange and methylene blue in water (see section 4, Figures S17–21 of SI), which do not suggest that **C2** is a suitable material for this application. Subsequent investigation also indicates **C2** is not fully stable in water. Crystals of **C2** that were soaked in water suffered some degradation in crystallinity however unit cell parameters could be determined using synchrotron radiation. Interestingly, the cell parameters obtained were a closer match to those of complex **C1a** than to **C2**, Table 1. Complex **C2** and **C1a** show extremely similar lattice packing as can be appreciated by comparison of Figure 4a and Figure 8a; and Figures S8a and S9. The main difference is the presence of the linear Cu-Cl-Cu bridge in **C2** which, in terms of lattice positions, corresponds to the  $\text{Cu-H}_2\text{O}\cdots\text{H}_2\text{O-Cu}$  hydrogen bonding that occurs between 1D coordination chains in **C1a**. Unfortunately, the crystal did not diffract sufficiently well for a full structure determination but this observation gives indirect evidence for the mechanism of the initial stage of hydrolysis of **C2** being the hydrolysis of the linear Cu-Cl-Cu bridges.

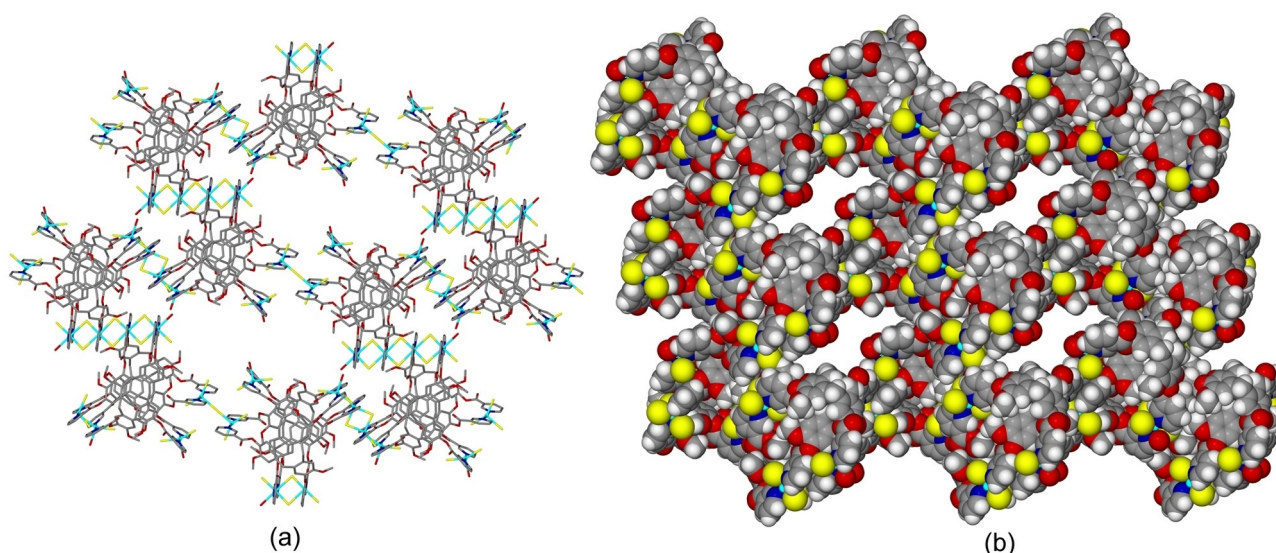


**Figure 8.** (a) 2D coordination polymer of **C2** (only one disorder position of terminal chloro of  $[\text{Cu}_2(\mu\text{-Cl})_6\text{Cl}_2]$  cluster is shown). (b) Space-filling view of 3D lattice of **C2** viewed down *b* axis, solvent molecules are not shown.

## Conclusions

A hitherto unreported type of cage-catenanes were obtained from the cyclotrimeratrylene-based ligand tris(nicotinoyl)cyclotriguaiacylene with Cu(II). The  $\{\text{Cu}_3(\text{L}1)_2\}$  metallo-cryptophane cage units are similar to previous reports of cage-catenanes but with additional copper chloride bridges between the two cages of the triply interlocked catenane. In all examples reported here, this copper chloride bridging motif extends to an unusual  $\{\text{Cu}_4(\mu\text{-Cl})_6\text{Cl}_2(\text{OH}_2)_2\}$  cluster that links two cage-catenane groups together into tetramer of metal-organic cages in a dimer of cage-catenanes motif. The originally obtained material formed through serendipitous scavenging of chloride contaminant, and this 0D material transforms to 1D coordination chain materials with further copper chloride bridges during solvent-exchange processes with concomitant uptake of toluene into the crystal lattice. A 2D coordination polymer obtained directly from L1 and  $\text{CuCl}_2$  shows a third copper chloride bridging motif, and unit cell measurements indicate this bridge is hydrolysed on exposure to water though with retention of a degree of crystallinity. Thus, both formation and dissociation of copper chloride bridges between the dimers of cage-catenanes can be prompted by solvent-exchange processes.

## Supporting Information

Details of synthetic procedures, spectroscopic, analytical and thermal characterisation, crystallographic information and additional figures of crystal structures. The authors have cited additional references within the Supporting Information (Ref. [40–42]). Data accessibility: data supporting this study are available at <https://doi.org/10.5518/1585>.

## Acknowledgements

MPS thanks the University of Leeds for a Gunnell and Matthews scholarship. This work was carried out with support of the Diamond Light Source award CY26879.

## Conflict of Interests

The authors declare no conflict of interest.

## Data Availability Statement

The data that support the findings of this study are openly available in University of Leeds library at <https://doi.org/10.5518/1585>, reference number 1585.

**Keywords:** catenane · metal-organic cage · coordination polymer · copper cluster · cyclotrimeratrylene

- [1] selected reviews: a) D. J. Bell, L. S. Natrajan, I. A. Riddell, *Coord. Chem. Rev.* **2022**, *472*, 214786; b) W.-T. Dou, C.-Y. Yang, L.-R. Hu, B. Song, T. Jin, P.-P. Jia, X. Ji, F. Zheng, H.-B. Yang, L. Xu, *ACS Materials Lett.* **2023**, *5*, 1061; c) T. Tateishi, M. Yoshimura, S. Tokuda, F. Matsuda, D. Fujita, S. Furukawa, *Coord. Chem. Rev.* **2022**, *467*, 214612; d) A. J. McConnell, *Chem. Soc. Rev.* **2022**, *51*, 2957; e) D. R. Martir, E. Zysman-Colman, *Chem. Commun.* **2019**, *55*, 139; f) S. Pullen, G. H. Clever, *Acc. Chem. Res.* **2018**, *51*, 3052; g) D. Zhang, T. K. Ronson, Y.-Q. Zou, J. R. Nitschke, *Nat. Chem. Rev.* **2021**, *5*, 168; h) A. J. McConnell, C. S. Wood, P. P. Neelakandan, J. R. Nitschke, *Chem. Rev.* **2015**, *115*, 7729; i) T. R. Cook, P. J. Stang, *Chem. Rev.* **2015**, *115*, 7001; j) K. Harris, D. Fujita, M. Fujita, *Chem. Commun.* **2013**, *49*, 6703, and references therein.
- [2] M. P. Snelgrove, M. J. Hardie, *CrystEngComm* **2021**, *23*, 4087, and references therein.
- [3] a) M. J. Hardie, *Chem. Lett.* **2016**, *45*, 1336; b) J. J. Henkelis, M. J. Hardie, *Chem. Commun.* **2015**, *51*, 11929, and references therein.
- [4] A. Collet, *Tetrahedron* **1987**, *43*, 5725.



- [5] Z. Zhong, A. Ikeda, S. Shinkai, S. Sakamoto, K. Yamaguchi, *Org. Lett.* **2001**, *3*, 1085.
- [6] recent examples a) E. Britton, M. J. Howard, M. J. Hardie, *Inorg. Chem.* **2021**, *60*, 12912; b) A. Schaly, M. Meyer, J.-C. Chambron, M. Jean, N. Vanthuyne, E. Aubert, E. Espinosa, N. Zorn, E. Leize-Wagner, *Eur. J. Inorg. Chem.* **2019**, *2019*, 2691; c) S. Oldknow, D. Rota Martir, V. E. Pritchard, M. A. Blitz, C. W. G. Fishwick, E. Zysman-Colman, M. J. Hardie, *Chem. Sci.* **2018**, *9*, 8150; d) V. E. Pritchard, D. Rota Martir, S. Oldknow, S. Kai, S. Hiraoka, N. J. Cookson, E. Zysman-Colman, M. J. Hardie, *Chem. Eur. J.* **2017**, *23*, 6290.
- [7] C. J. Bruns, J. F. Stoddart, *The Nature of the Mechanical Bond: From Molecules to Machines*, John Wiley & Sons, Inc., Hoboken, NJ, USA, **2016**, 10.1002/9781119044123.
- [8] reviews a) S. Bai, Y.-F. Han, *Acc. Chem. Res.* **2023**, *56*, 1213; b) M. Frank, M. D. Johnstone, G. H. Clever, *Chem. Eur. J.* **2016**, 22 and references therein.
- [9] recent examples: a) H.-M. Yu, M.-H. Du, J. Shu, Y.-H. Deng, Z.-M. Xu, Z.-W. Huang, Z. Zhang, B. Chen, P. Braunstein, J.-P. Lang, *J. Am. Chem. Soc.* **2023**, *145*, 25103; b) D. Chakraborty, R. Saha, J. K. Clegg, P. S. Mukherjee, *Chem. Sci.* **2022**, *13*, 11764; c) Y. Wu, Q.-H. Guo, Y. Qiu, J. A. Weber, R. M. Young, L. Bancroft, Y. Jiao, H. Chen, B. Song, W. Liu, Y. Feng, X. Zhao, X. Li, L. Zhang, X.-Y. Chen, H. Li, M. R. Wasielewski, J. F. Stoddart, *Proc. Natl. Acad. Sci. USA* **2022**, *119*, e2118573119; d) Y.-Y. Zhang, F.-Y. Qiu, H.-T. Shi, W. Yu, *Chem. Commun.* **2021**, *57*, 3010; e) W. Yu, F.-Y. Qiu, S.-T. Luo, H.-T. Shi, G. Yuan, X. Wei, *Inorg. Chem. Front.* **2021**, *8*, 2356; f) Y. Wang, Y. Zhang, Z. Zhou, R. T. Vanderlinden, B. Li, B. Song, X. Li, Lei Cui, X. Jia, J. Fang, C. Li, P. J. Stang, *Nat. Commun.* **2020**, *11*, 2727; g) Y.-W. Zhang, S. Bai, Y.-Y. Wang, Y.-F. Han, *J. Am. Chem. Soc.* **2020**, *142*, 13614; h) T. R. Schulte, J. J. Holstein, L. Schneider, A. Adam, G. Haberhauer, G. H. Clever, *Angew. Chem. Int. Ed.* **2020**, *59*, 22489; i) T. K. Ronson, Y. Wang, K. Baldrige, J. S. Siegel, J. R. Nitschke, *J. Am. Chem. Soc.* **2020**, *143*, 10267; j) A. Kumar, P. S. Mukherjee, *Chem. Eur. J.* **2020**, *26*, 4842; k) T. Tateishi, Y. Yasutake, T. Kojima, S. Takahashi, S. Hiraoka, *Commun. Chem.* **2019**, *2*, 25; l) S.-Z. Zhan, J.-H. Li, G.-H. Zhang, X.-W. Liu, M. Li, J. Zheng, S. W. Ng, D. Li, *Chem. Commun.* **2019**, *55*, 11992; m) L. Yang, X. Jing, B. An, C. He, Y. Yang, C. Duan, *Chem. Sci.* **2018**, *9*, 1050–1057.
- [10] M. Fujita, N. Fujita, K. Ogura, K. Yamaguchi, *Nature* **1999**, *400*, 52.
- [11] Y. Yamauchi, M. Yoshizawa, M. Fujita, *J. Am. Chem. Soc.* **2008**, *130*, 5832.
- [12] A. Westcott, J. Fisher, L. P. Harding, P. Rizkallah, M. J. Hardie, *J. Am. Chem. Soc.* **2008**, *130*, 2950.
- [13] J. J. Henkelis, T. K. Ronson, L. P. Harding, M. J. Hardie, *Chem. Commun.* **2011**, *47*, 6560.
- [14] a) L. Cheng, C. Liang, W. Liu, Y. Wang, B. Chen, H. Zhang, Y. Wang, Z. Chai, S. Wang, *J. Am. Chem. Soc.* **2020**, *142*, 16218; b) X. Kuang, X. Wu, R. Yu, J. D. Donahue, J. Huang, C.-Z. Lu, *Nat. Chem.* **2010**, *2*, 461.
- [15] L. Jiang, P. Ju, X.-R. Meng, X.-J. Kuang, T.-B. Lu, *Sci. Rep.* **2012**, *2*, 668.
- [16] a) J. Martí-Rujas, S. Elli, A. Famulari, *Sci. Rep.* **2023**, *13*, 5605; b) A. Famulari, J. Martí-Rujas, *Cryst. Growth Des.* **2022**, *22*, 4494; c) Q. Chen, F. Jiang, D. Yuan, L. Chen, G. Lyu, M. Hong, *Chem. Commun.* **2013**, *49*, 719; d) J. Heine, J. Schmedt auf der Günne, S. Dehnen, *J. Am. Chem. Soc.* **2011**, *133*, 10018.
- [17] Z. Sun, P. Li, S. Xu, Z.-Y. Li, Y. Nomura, Z. Li, X. Liu, S. Zhang, *J. Am. Chem. Soc.* **2020**, *142*, 10833.
- [18] a) W. M. Bloch, J. J. Holstein, B. Dittrich, Wolf Hiller, G. H. Clever, *Angew. Chem. Int. Ed.* **2018**, *57*, 5534; b) R. Zhu, I. Regeni, J. J. Holstein, B. Dittrich, M. Simon, S. Prévost, M. Gradzielski, G. H. Clever, *Angew. Chem. Int. Ed.* **2018**, *57*, 13652.
- [19] M. J. Hardie, R. M. Mills, C. J. Sumbly, *Org. Biomol. Chem.* **2004**, *2*, 2958.
- [20] Deposition Numbers 2387083 (for C1), 2387084 (for C1a), 2387085 (for C1b) and 2387086 (for C2) contain the supplementary crystallographic data for this paper. These data are provided free of charge by the joint Cambridge Crystallographic Data Centre and Fachinformationszentrum Karlsruhe Access Structures service.
- [21] T. K. Ronson, M. J. Hardie, *CrystEngComm* **2008**, *10*, 1731.
- [22] Example of cage-catenane linked through metal coordination: Y. Li, H. Jiang, W. Zhang, X. Zhao, M. Sun, Y. Cui, Y. Liu, *J. Am. Chem. Soc.* **2024**, *146*, 3147.
- [23] Y. Han, Y. Song, *Inorg. Chem. Commun.* **2015**, *55*, 83.
- [24] D. J. Carnevale, L. N. Dawe, C. P. Landee, M. M. Turnbull, J. L. Wikaira, *Polyhedron* **2021**, *202*, 115200.
- [25] for example a) K. E. Halvorson, T. Grigereit, R. D. Willet, *Inorg. Chem.* **1987**, *26*, 1716; b) R. D. Willett, U. Geiser, *Inorg. Chem.* **1986**, *25*, 4558.
- [26] a) N. Komiya, T. Naota, S. Murahashi, *Tetrahedron Lett.* **1996**, *37*, 1633; b) J.-V. Folgado, P. Gomez-Romero, F. Sapina, D. Beltran-Porter, *J. Chem. Soc., Dalton Trans.* **1990**, 2325.
- [27] J. Poitras, M. Leduc, A. L. Beauchamp, *Can. J. Chem.* **1993**, *71*, 549.
- [28] J. W. Weenk, A. L. Speck, *Cryst. Struct. Commun.* **1976**, *5*, 805.
- [29] S. Menson, M. V. Rajasekharan, J.-P. Tuchagues, *Inorg. Chem.* **1997**, *36*, 4341.
- [30] O. V. Dolomanov, L. J. Bourhis, R. J. Gildea, J. A. K. Howard, H. Puschmann, *J. Appl. Crystallogr.* **2009**, *42*, 339.
- [31] F. L. Thorp-Greenwood, T. K. Ronson, M. J. Hardie, *Chem. Sci.* **2015**, *6*, 5779.
- [32] E. Fernandez-Bartolome, A. Martinez-Martinez, E. Resines-Urien, L. Piñero-Lopez, J. S. Costa, *Coord. Chem. Rev.* **2022**, *462*, 214281, and references therein.
- [33] first example B. F. Abrahams, M. J. Hardie, B. F. Hoskins, R. Robson, G. A. Williams, *J. Am. Chem. Soc.* **1992**, *114*, 10641.
- [34] S. Krause, N. Hosono, S. Kitagawa, *Angew. Chem. Int. Ed.* **2020**, *59*, 15325, and references therein.
- [35] Y.-Q. Lan, H.-L. Jiang, S.-L. Li, Q. Xu, *Inorg. Chem.* **2012**, *51*, 7484.
- [36] A. N. Khlobystov, N. R. Champness, C. J. Roberts, S. J. B. Tandler, C. Thompson, M. Schröder, *CrystEngComm* **2002**, *4*, 426.
- [37] a) S. Kim, I.-H. Park, H.-B. Choi, H. Ju, E. Lee, T. S. Herng, J. Ding, J. H. Jung, S. S. Lee, *Dalton Trans.* **2020**, *49*, 1365; b) A. Nielsen, S. Veltzé, A. D. Bond, C. J. McKenzie, *Polyhedron* **2007**, *26*, 1649; c) F. Uguzzoli, C. Massera, A. M. M. Lanfredi, N. Marsich, A. Camus, *Inorg. Chim. Acta* **2002**, *340*, 97; d) R. A. Bauer, W. R. Robinson, D. W. Margerum, *J. Chem. Soc., Chem. Commun.* **1973**, 289.
- [38] A. Ray, D. Maiti, W. S. Sheldrick, H. Mayer-Figge, S. Mondal, M. Mukherjee, S. Gao, M. Ali, *Inorg. Chim. Acta.* **2005**, *358*, 3471.
- [39] for example: a) Somnath, M. Ahmad, K. A. Siddiqui, *ACS Omega* **2022**, *45*, 41120; b) L.-X. Ma, W.-J. Zhou, L.-Y. Li, M. Zha, B.-L. Li, B. Wu, C.-J. Hu, *J. Solid State Chem.* **2022**, *316*, 123615; c) T. Wen, D.-X. Zhang, J. Zhang, *Inorg. Chem.* **2012**, *52*, 12.
- [40] a) G. M. Sheldrick, *Acta Crystallogr.* **2015**, *A71*, 3; b) G. M. Sheldrick, *Acta Crystallogr.* **2015**, *C71*, 3.
- [41] B. Rees, L. Jenner, M. Yusupov, *Acta Crystallogr.* **2005**, *D61*, 1299.
- [42] L. J. Barbour, *J. Appl. Crystallogr.* **2020**, *53*, 1141.

Manuscript received: October 4, 2024  
Accepted manuscript online: December 10, 2024  
Version of record online: December 19, 2024